Time Series Remote Sensing Data-Based Identification of the Dominant Factor for Inland Lake Surface Area Change: Anthropogenic Activities or Natural Events?

Xiaolong Liu [1,2], Zhengtao Shi [1,2]*, Guangcai Huang [1], Yanchen Bo [4], Guangjie Chen [1,3]

[1] College of Tourism & Geography Science, Yunnan Normal University, Kunming 650500, Yunnan, China; liuxl@ynnu.edu.cn (X.L.); Guangcai2020@163.com (G.H.); guangjiechen@gmail.com (G.C.)
[2] Key Laboratory of Environmental Change on Lower Latitude Plateau for Universities in Yunnan Province, Kunming 650500, Yunnan, China;
[3] Provincial Key Laboratory of Plateau Geographical Processes & Environmental Change, Kunming 650500, Yunnan, China;
[4] Faculty of Geographical Science, Beijing Normal University, Beijing 100875, China; boyc@bnu.edu.cn (Y.B.)
* Correspondence: shizt@ynnu.edu.cn; Tel.: +86-13187824966.

Abstract: Inland lake variations are considered sensitive indicators of global climate change. However, human activity is playing as a more and more important role in inland lake area variations. Therefore, it is critical to identify whether anthropogenic activity or natural event is playing as the dominant factor in inland lake surface area change. In this study, we proposed a Douglas-Peucker simplification algorithm and bend simplification algorithm combined method to locate major lake surface area disturbances; these disturbances were then characterized to extract the time series change features according to documented records; and the disturbances were finally classified into anthropogenic or natural. We took the nine lakes in Yunnan Province as test sites, a 31 years long (from 1987 to 2017) time series Landsat TM/OLI images and HJ-1A/1B used as data sources, the official records was used as references to aid the feature extraction and disturbance identification accuracy. Results of our method for both disturbance location and the disturbance identification could be concluded as follows: 1) The method can accurately locate the main lake changing events based on the time series lake surface area curve. The accuracy of this model for segmenting the lake area time series curves in our study area was 95.24%. 2) Our proposed method achieved an overall accuracy of 91.67%, with F-score of 94.67 for anthropogenic disturbances and F-score of 85.71 for natural disturbances. 3) According to our results, lakes in Yunnan Provence, China, have undergone extensive disturbances, and the human-induced disturbances occurred almost twice as often as natural disturbances, indicating intensified disturbances caused by human activities. This inland lake area disturbance identification method is expected to uncover whether a disturbance to inland lake area is human activity-induced or natural event.

Keywords: time series; lake changes; remote sensing; inland lake; lake disturbance

1. Introduction

Inland lakes are important aspects of land surface cover that participate in the natural water cycle and are considered highly sensitive to the impacts of climate change and human activities [1–2]. Shrinkage or extension of inland lakes can reflect global climate and environment changes [3]. Thus, inland lake variations are considered sensitive indicators of global climate change [4–5]. Most lake variations are caused by natural events or anthropogenic activities. However, these variations are mostly documented by the local authorities or institutions and are rarely obtained from remote sensing technology.

This study focuses on remote sensing methods to identify the dominant factors affecting changes to inland lake surface area. With advantages of wide coverage, high frequency data collection, labor and economic cost-effectiveness, remote sensing technology has been used in previous lake change studies [6–8], especially for lakes located in remote and less developed areas where lake surface changes have been only rarely documented [2].

With ongoing earth observation projects (such as NASA's Earth Observing System (EOS) and the European Union's Copernicus program) and the development of sensors (from visible to infrared and SAR), times series lake observation data are providing new means to study lake change. Remote sensing data used for lake monitoring could be divided into three categories according to their spatial resolution: coarse-, medium- and high-spatial resolution data. Although coarse spatial resolution remote sensing data (such as NOAA/AVHRR, MODIS, Suomi NPP-VIIRS and Sentinel-3) have lower spatial resolution and inherent defects, they often have higher revisit frequency and a wider coverage; therefore, they have been widely used in water monitoring [9–10]. For example, Che et al. [11] applied the synthesized monthly MODIS09A1 data to extract the lake area of the Qinghai-Tibet Plateau from 2000 to 2013 using the synthesized NDWI and NDWI water body index proposed by Mcfeeters [12]; the results showed that the lake area of the Qinghai-Tibet Plateau significantly expanded during 2000 and 2013. Using time series MODIS data to identify Poyang lake water area changes, Feng et al. [13] found that Poyang Lake had significant seasonal and interannual changes during 2000 and 2010, mainly due to the influence of climate fluctuations. With the development of better sensors, high spatial resolution land monitoring satellites, such as QuickBird, IKONOS, Worldview, RapidEye, ZY-3, GF-1/2, can provide more accurate and higher spatially resolved land cover observations. However, the small image coverage and the long revisit periods of high spatial resolution data remain obstacles for the detection of change in larger inland water bodies [6].

Among these three kinds of data, the medium-resolution data, such as Landsat, HJ-1A/B, ASTER, and Sentinel-2 data, are the most widely used in water monitoring applications. The main reason for their frequency of use is the free data access policy and the long-term monitoring of Earth's surface changes that these datasets represent; e.g., Landsat data includes continuous observations of up to 40 a [14–16]. A wide range of studies have been employed to study changes to the lake surfaces using medium-resolution remote sensing data. For example, in order to obtain the water area of the Yunnan-Guizhou Plateau from 1985 to 2015, Xiao et al. [17] extracted lake surface areas using Landsat image data from 5 periods at 5 a intervals and found that the water area of lakes in the Yunnan-Guizhou Plateau first increased and then decreased during this period. Tulbure et al. [8] studied the relationship between water body areas and changes in the weather in the Murray-Darling Basin and the Barmah-Millewa forests from 1986 to 2011; the results show that extreme weather events, such as drought and rainfall, have a significant impact on surface water bodies and submergence dynamics. Using Landsat time series data, Arvor et al. [18] developed a method for automatically identifying small water bodies and used it to extract the area and quantity of small reservoirs in the Amazon region of southern Brazil from 1985 to 2015. The results show that the total area and quantity of small reservoirs in the area increased by 10 times and more than 5 times during the study period, respectively.

In summary, existing remote sensing technology used in inland water body identification with median spatial resolution has provided reliable results for monitoring inland lake change. However, most inland lakes are affected by human activities, and few studies have tried to identify the dominant factor affecting inland lake surface change based on remote sensing data: human activities or natural events? This identification is critical for uncovering the relationship between human activities and the natural environment on both local and global scales. Thus, in this study, we take 9 large inland lakes on the Yunnan Plateau for our study area and apply the proposed time series lake surface area change analysis method to uncover changes in inland lakes and to identify whether human activities or natural events dominate these changes.

2. Study Area and Data

Peer-reviewed version available at Remote Sens. 2020, 12, 612; doi:10.3390/rs12040612

2.1 Overview of study area

The Yunnan Plateau is part of the Yunnan-Guizhou Plateau, which is one of the four major plateaus in China. This area is located in southwest China and is characterized by rough terrain and a subtropical monsoon climate. There are many inland lakes on the Yunnan-Guizhou Plateau; lakes here play important roles in the ecological environment and regional water security and even have been considered important strategic resources for the state economy and social development.

There are more than 40 lakes that vary in size on the Yunnan Plateau and lake basins are where industry and agriculture activities are mostly concentrated. The nine lakes selected for this study are located in different areas with varied geographical environments in Yunnan Province (Figure 1) and include 5 faulted tectonic lakes (Dianchi and Qilu, Erhai, Haixi, and Bita), 1 faulted karst lake (Lashi), 1 structural faulted glacial lake (Shudu) located in northwest Yunnan, and 2 karst lakes (Yilong and Yuxian) located in south and southeast Yunnan. The nine lakes span the subtropical alpine monsoon climate zone, the low-latitude warm temperate zone plateau mountain monsoon climate, and the plateau cold and warm humid climate. The elevation of Yunnan Province varies from 1,420 m.a.s.l. to 3,620 m.a.s.l. Among the nine lakes, Dianchi Lake, known as the "Plateau Pearl," is the largest freshwater lake in Yunnan Province; Yuxian Lake completely dried out in several years according to surveys by [19]. The surface area of this lake rapidly decreased to approximately 150 m2 in August 2013 and the lake had completely dried up when a survey was conducted again in March 2014 by Hu Kui. Qilu Lake and Yilong Lake are undergoing severe anthropogenic disturbance, and Bita Lake is currently being subjected to minimal anthropogenic disturbance. These lakes are distributed in different regions and at different elevations and are therefore highly representative.

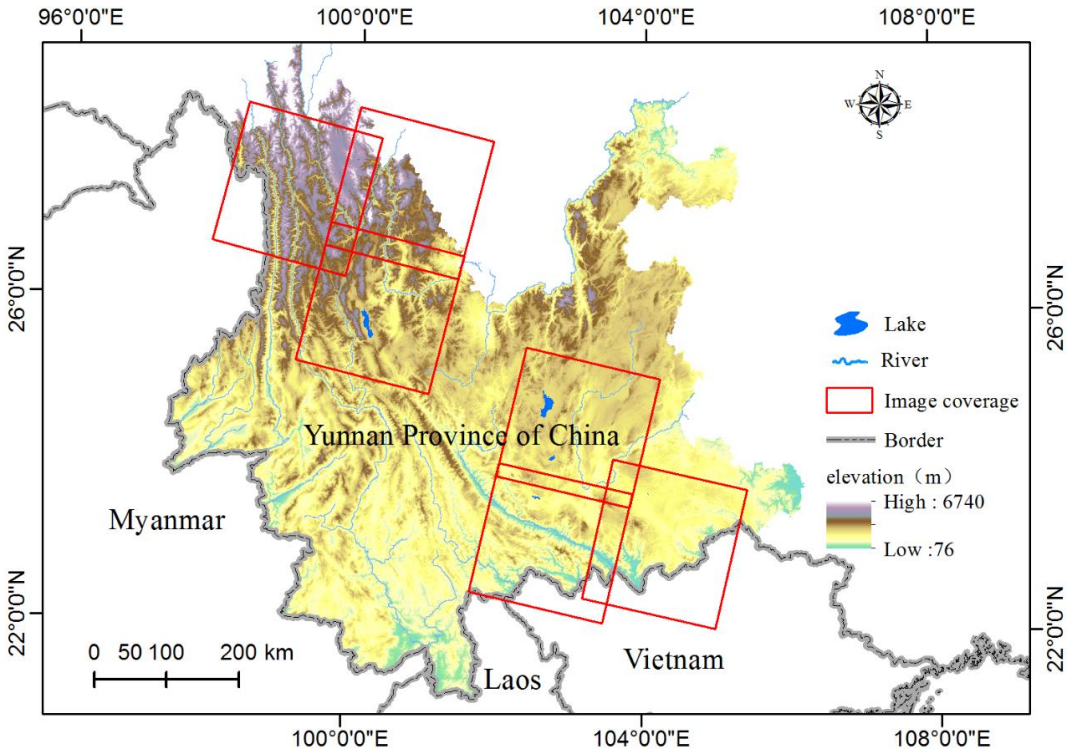

Figure 1. Overview of the study area.

2.2 Data source and preprocessing

In this study, Landsat TM/OLI remote sensing image data with a time span of 31 years (1986–2017) were used as the main data source for extracting lake surface area. Due to the malfunction of the Landsat-7 ETM+ scanning line corrector, there were no usable Landsat data for this study area during the time period between November 3, 2011 and April 12, 2013, expect for ETM+. Therefore,

we used HJ-1A/B CCD data, which has the same spatial resolution as the Landsat data (30 m spatial resolution), to supplement the missing Landsat data during this period. The level-1 Landsat data were downloaded from the United States Geological Survey website (https://glovis.usgs.gov/) and the HJ-1A/B data were downloaded from the China Centre for Resources Satellite Data and Application (CRESDA) (http://www.cresda.com/). Because of the distinct dry and wet seasons in Yunnan Province, approximately 90% of the year's precipitation is concentrated in the rainy season (from May to October of a year), while only 10% occurs during the dry season (from November to the next April) [20]. In addition, because the available remote sensing image data for the rainy season in this study area are very limited, the remote sensing data were all selected from the period between November and the next April to ensure that there was at least one available Landsat observation for each year. A total of 795 Landsat level-1 images were downloaded, covering 6 different scenes (see Table 1 for details). In addition, 27 HJ-1A/B images were used, and each of the selected images was cloud-free over the lakes in the study area.

Remote sensing data used in this study were preprocessed, which included radiation calibration, atmospheric correction, and geometric correction. For the atmosphere correction of Landsat data, the FLAASH (Fast Line-of-sight Atmospheric Analysis of Spectral Hypercubes) model, which is based on the ModTRAN model on ENVITM 5.3 software, was used to create the Landsat-based surface reflectance data [21]. Because clouds and cloud shadows are obstacles to optical remote sensing data-used classification, the Fmask algorithm provided by Zhu was used to remove the clouded and shadowed pixels [22], and the removed pixels were filled with the nearest available data. The radiation calibration and atmospheric correction of the HJ-1A/B data were also performed using ENVITM 5.3 software. The calibration parameters and spectral response functions required for the radiation calibration and the atmospheric correction of the HJ1A/B data were obtained from the China Centre for Resources Satellite Data and Application CRESDA website (http://www.cresda.cn/CN/Downloads/dbcs/index.shtml). In addition, Landsat orthophoto images were used as reference images to register the HJ-1A/B data, and approximately 16 ground control points were uniformly selected for each image. The polynomial model and the nearest neighbor resampling methods were used to correct the HJ-1A/B data.

Table 1. Remote sensing images used in this study

Date	Satellite Sensors	Number of Images selected	Spatial Resolution	Data Source
11/01/1986-11/02/2011	Landsat TM	686	30 m	https://glovis.usgs.gov/
11/03/2011-04/12/2013	HJ-1A/B	27	30 m	http://www.cresda.com/
04/13/2013-04/30/2017	Landsat OLI	109	30 m	https://glovis.usgs.gov/

3. Methods

Climate variability and human interventions are commonly considered two major contributors to variations in inland lakes [23]. To identify lake disturbances that are dominated by different factors using time series remote sensing data, this paper proposes a lake disturbance identification algorithm that consists of two parts: the first is the Douglas-Peucker algorithm [24] and bend simplification algorithm [25] to segment the Landsat data derived time series lake surface area curve. Second, according to the documented lake surface area change records, the characteristics of the change in the main lake surface in the time series curve are summarized and the classification features are extracted to identify the main lake surface area change events. The specific steps are as follows: 1) time series lake surface area curve construction; 2) curve simplification following the Douglas-Peucker algorithm; 3) bend simplification to further simplify the segmented time series curve; and 4) feature extraction and event identification.

3.1 Lake surface extraction and time series lake surface area curve construction

Many inland water body identification methods have been developed since the emergence of remote sensing technology. However, among these methods, the water index-based method has proven to be simple and effective for extracting the water body [26–28].

Widely used water indices include the normalized difference water index (NDWI), modified normalized difference water index (MNDWI), enhanced water index (EWI), automated water extraction index (AWEI), multiband water index (MBWI), and WI2015 [29]. In particular, the NDWI and MNDWI are the most widely used [6]. Therefore, in this study, we adopted the MNDWI index combined with the Otsu algorithm to adaptively determine the optimum segmentation threshold for extracting lake areas from the Landsat images. The Otsu method [30] algorithm proposed by Otsu is a type of self-adaptive thresholding method that is also referred to as the maximum interclass variance method and is derived by least square estimation. The Otsu method used in this study will exclude the influence of mis-segmentation to water and non-water areas due to artificially set thresholds to the MNDWI.

The MNDWI that was obtained by Xu [31] by revising the waveband combination of the NDWI is one of the most typical and most widely used methods for water extraction. The basic principle of this index is that the reflectivity of water in the mid-infrared band continues to decrease, while the reflectivity of ground features, such as soil and buildings, abruptly increases from the near-infrared band to the mid-infrared band. This pattern greatly reduces confusing water and buildings, reduces the background noise, and benefits the extraction of thematic information about the water. Therefore, in this study, we use the MNDWI (see formula (1)) to extract water bodies, as follows:

$$NDWI = \frac{Green - MIR}{Green + MIR} \quad (1)$$

where Green represents the green light band and MIR represents the mid-infrared band.

The single-band threshold method was used to extract water from the HJ-1A/1B images. After PC (principal component) transformation of the HJ-1A/1B data, a significant difference between water and non-water was maximized on the 2nd component (or band) [32]. Thus, by selecting an appropriate threshold, water information can be satisfactorily extracted using the single-band method.

Analysis of a time series curve plotted with sufficiently continuous lake area data not only effectively reflects the lake area variation trend but also captures any major lake disturbance events. In this study, the input data used to construct the time series curve were the annual average lake area measurements extracted from the remote sensing images during each dry season (November to April of the next year) from 1987 to 2017.

3.2 Time series lake surface area curve segmentation and identification of disturbance events

(1) Simplification of the time series curve using the Douglas-Peucker algorithm

The occurrence of large natural or human activities in (or around) a lake will cause lake area disturbances. For example, dam construction or water storage in a lake will cause a sudden increase in lake area, whereas land reclamation around a lake will cause a rapid decrease in lake area. Furthermore, strong natural events such as rainfall or drought can also cause increases or decreases in lake area. Such event-induced lake changes manifest as sudden changes in the time series lake surface area curve. However, minor events or precipitation differences will also cause variations in the time series curve. These changes are not key factors affecting the lake area but may be obstacles to the identification of key disturbances; thus, they are considered noise that should be removed for the time-series analysis.

Several methods, such as LandTrendr [33], CCDC [34], and BFAST [35], have been proposed to identify disturbances using remotely sensed time series indices (such as the NDVI (Normalized

Difference Vegetation Index), NBR (Normalized Burn Ratio), TCA (Tasselled Cap Angle). However, most of the lake surface area time series appear to be purely random and nonstationary time series (see Table 2); unlike indices such as NDVI, NBR, and TCA, lake surface areas are dimensionless, which means existing models are theoretically unsuitable for the analysis of lake surface area time series. Fortunately, the Douglas-Peucker (D-P) line simplification algorithm, which is used to eliminate low-intensity noises and smooth minor changes on the curve to better capture larger changes on the curve, is an appropriate alternative.

Table 2. Stability test by the Ad test to lake surface area time series of the 9 lakes.

Lake	Ad Test (at 0.05 level)	Stationary (yes/ no)
Shudu lake	P=0.5355 > 0.05	no
Qilu Lake	P=0.341 > 0.05	no
Yilong Lake	P=0.1825 > 0.05	no
Bitahai Lake	P=0.03192 < 0.05	yes
Lashihai Lake	P=0.04617 < 0.05	yes
Yuxian Lake	P=0.3644 > 0.05	no
Haixihai Lake	P=0.5563 > 0.05	no
Dianchi Lake	P=0.01 < 0.05	yes
Erhai Lake	P=0.1577 > 0.05	no

The D-P algorithm was proposed by Douglas and Peucker in 1973 [24]. Currently, this algorithm is recognized as a classical algorithm for vector line simplification in GIS (geographic informational system). The basic idea of the algorithm is as follows: 1) line AB (see Figure 2) connects the two end points A and B of a time series curve, forming the chord of the curve; 2) for each of the points (for example, point C) between A and B on the curve, there will be a distance to this chord (to line AB), forming a set of distances D, and the maximum distance of D is d(max); 3) d(max) is then compared with the given tolerance ε, and if d(max) is smaller than ε, then line AB is taken to be the approximation of the curve, and the processing of this curve section ends, but if d(max) is larger than ε, then the corresponding point (point C) is used to divide the curve into two subsegments (AC and BC), and each of the two subsegments is further processed following steps 1 through 3 until each of their d(max) values is less than the given ε; and 4) after all the curves are processed, the segmentation points are connected sequentially to form a polyline that represents a simplification of the curve.

Preprints (www.preprints.org) | NOT PEER-REVIEWED | Posted: 30 December 2019 doi:10.20944/preprints201912.0392.v1

Peer-reviewed version available at Remote Sens. 2020, 12, 612; doi:10.3390/rs12040612

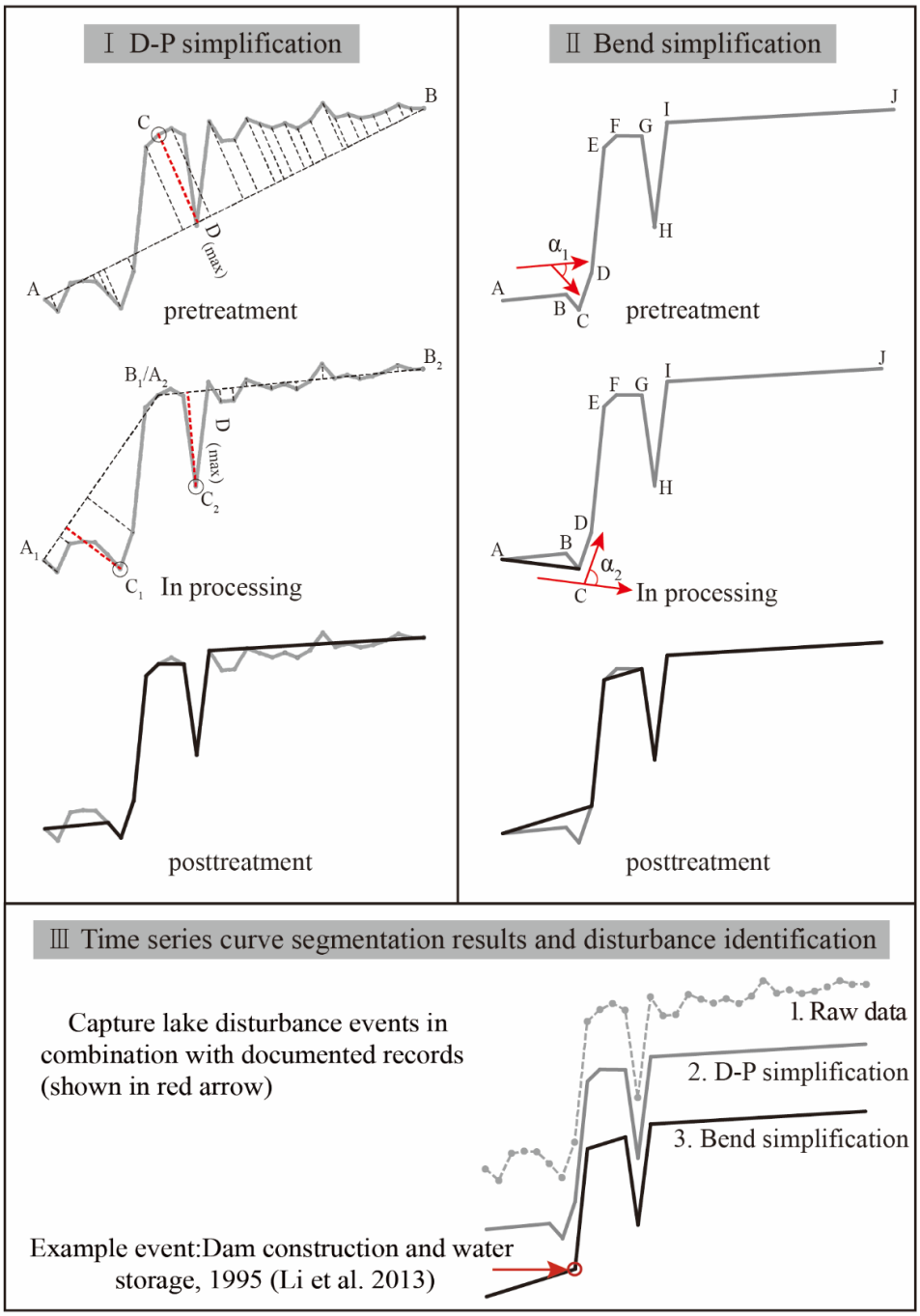

Figure 2. Segmentation method for time series curves.

(2) Bend simplification and time series curve segmentation

After D-P simplification of the time series curve, several minor-change points may not have been removed. As these points are not indicative of major lake disturbance events, they should be removed. To retain only the feature points with the main fluctuations on time series curves, we use the bend simplification algorithm, which can eliminate smaller fluctuations [36], to simplify the D-P algorithm simplified curve.

The bend simplification algorithm is used to determine whether the variation in the curvature at each point is smooth. Given a predefined threshold, if the curvature is smaller than the threshold, then the point will be eliminated and a new segment will be created between the two points adjacent to the eliminated point. However, if the curvature exceeds the predefined threshold, the corresponding point will be considered a potential feature point and will be retained. After each point

is processed, the retained potential points are then connected sequentially to form the finally simplified time series curve. The specific steps of the bend simplification algorithm are illustrated in Figure 2 and are explained as follows: 1) first, we calculate the curvatures on each point of the curve except for the first and last points; 2) second, for the curvature on the second point (for example point B), the two adjacent points A and C are used to construct vectors AB and BC, and the angle formed by these two vectors is calculated as $\alpha 1$; if $\alpha 1$ is larger than the preset threshold α, the curvature on point B is considered to be large and will be retained as a key point; however, if the angle $\alpha 1$ between vector AB and BC is less than the preset threshold α, point B will be removed. Following the steps above, curvatures on point C, D, etc. will be judged one by one; 3) after step 2), all points, except the beginning and the end points, that meet the given curvature threshold α are retained as feature points that are representative of the main lake surface area change events.

(3) Feature extraction and disturbance identification

After the segmentation of the time series curve of the lake area, the lake surface area disturbance events that occurred during the long-term change of the lake will be obtained (known as the trajectory); each segment represents different lake disturbance events, and the beginning of a segment is usually the year in which the corresponding disturbance occurred, and the end corresponds to the year in which the disturbance ended. When the lake is greatly disturbed by external influences, the variation in the lake area time series curve segmentation reflects this and the lake disturbance features caused by different leading factors in the time series curve are also quite distinguishable. To accurately classify the identified lake disturbance events based on the segmentation results, 23 lake disturbance events recorded in 9 lakes in the study area were divided into two groups; one group was used to establish the lake disturbance classification rules, while the other group was used to verify the accuracy of the classification results.

Unlike trajectory classifications of disturbances in forests, lake disturbance classifications are small sample-based classification tasks, because major lake surface area disturbances are small probability events that cause training sample insufficiency of classifiers, such as statistical classifiers, machine learning classifiers or artificial intelligence classifiers. In addition, the binary classification problem in this study is to classify disturbances into anthropogenic or natural events. By analyzing each type of disturbance and its time series curve features, we find that there are strong relationships between the disturbance types and their curve changing trajectory. Therefore, we used a decision rule based disturbance type identification method to classify disturbances into anthropogenic or natural events. The decision rules for each node are based on the features extracted, as described above.

This study followed the CART (Classification and Regression Trees) method developed by Breiman [37]. The CART method classifies samples into a predefined number of classes by splitting learning samples into smaller parts following a set of rules at each split node. The CART is robust for isolating outliers in an individual node or nodes [38]. The splitting algorithm that maximizes the difference at each node through all possible values of variables is key for building the CART method. One of the most widely used splitting rules is the Gini splitting rule, given as follows:

$$\text{Gini Index} = 1 - \sum_{i=1}^{c} p_i^2 \quad (2)$$

where p_i is the conditional probability of class i in a training sample S that will be correctly classified, and C is the number of classes (anthropogenic or natural disturbances in this study). A lower Gini indicates the greater separability for that node, and the Gini will be calculated at each node using the specified features of lake surface area change. The features used in the CART method includes the amplitude of a disturbance, its duration, and the curve shape formed by the changing and recovering process. If one of the features (F for instance) has a minimum Gini value, then the training sample S will be split into S_1 and S_2 by Equation 3, as follows:

$$Gini_F = \frac{|S_1|}{S}\text{Gini}(S_1) + \frac{|S_2|}{S}\text{Gini}(S_2) \quad (3)$$

4. Results and discussion

4.1. Accuracy evaluation of extracted lake surface area

The water storage of inland lakes significantly changes seasonally, and it is not possible to accurately obtain in situ measurements of the lake surface area for each remotely sensed image. Moreover, visual interpretation would result in the confusion between lake boundary and water body. However, the satellite borne synthetic aperture radar (SAR) system with longer working bands makes the radar image have all-weather imaging capability, and several sensors (such as Sentinel-1, RADARSAT, TanDEM-X, TerraSAR-X) have high spatial resolution, which can greatly improve land cover detection efficiency and accuracy [39]. The Sentinel-1A data are the first radar data in the history of SAR that are publicly available for free download (https://vertex.daac.asf.alaska.edu/). With a 12 day revisit capability and 10 m spatial resolution, the Sentinel-1 SAR data was chosen as the validation data to assess the lake extraction accuracy. To minimize the influence of seasonal precipitation, the Sentinel-1 data with the closest imaging time to Landsat images were selected to validate the lake surface area extraction accuracy.

The SAR and the MNDWI-based lake surface area extraction results of the 9 chosen lakes are shown in Table 3. Compared with the Sentinel-1 data extracted lake areas, the maximum bias was 0.0918% for Lashihai Lake and the minimum bias was 0.0016% for Shudu Lake, and each of the 9 lakes had a bias of less than 0.1% between the Sentinel-1 and the OLI extracted results. The extracted annual lake area data with a small bias and the Sentinel-1 extracted lake areas were used to establish a reliable time series curve. Landsat-derived lake surface areas are presented in Figure 3.

Table 3. Accuracies of different lake water extraction results.

Lakes	Landsat-OLI	Area(km²)	Sentinel-1A	Area(km²)	Area differences (km²)
Shudu Lake	02/15/2017	1.69020	02/10/2017	1.68757	0.00263
Qilu Lake	03/14/2017	32.1237	03/13/2017	30.9925	1.1312
Yilong Lake	03/14/2017	18.2070	03/13/2017	17.3267	0.8803
Bitahai Lake	02/15/2017	1.61190	02/10/2017	1.59107	0.02083
Lashihai Lake	02/03/2015	12.2823	01/30/2015	11.2494	1.0329
Yuxian Lake	03/23/2017	0.95760	03/22/2017	0.91313	0.04447
Haixihai Lake	02/08/2017	3.76830	02/10/2017	3.54764	0.22066
Dianchi Lake	03/14/2017	298.323	03/13/2017	295.423	2.9
Erhai Lake	02/08/2017	242.337	02/10/2017	241.348	0.989

Peer-reviewed version available at Remote Sens. 2020, 12, 612; doi:10.3390/rs12040612

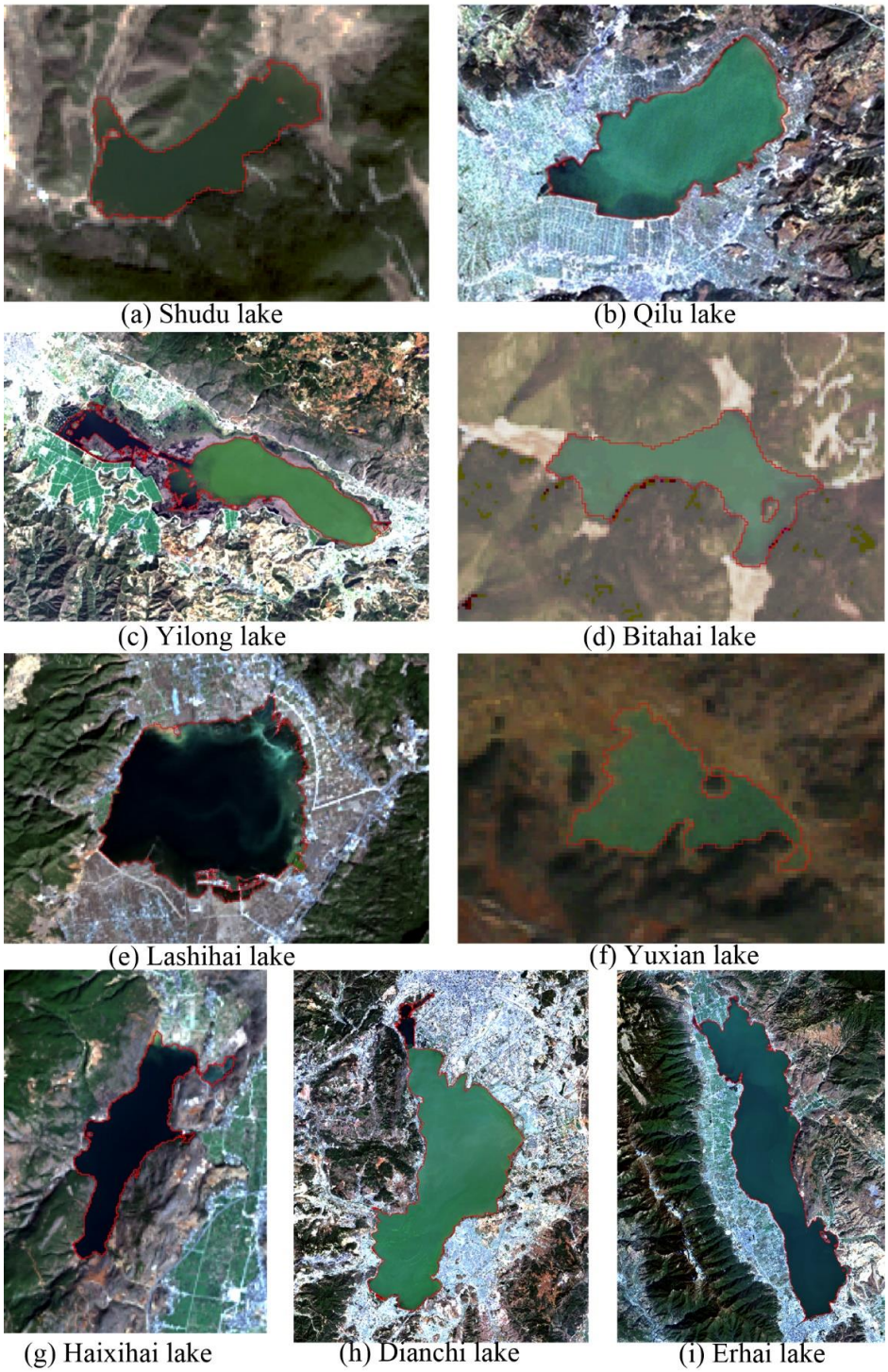

Figure 3. The 9 lakes and their extracted boundaries (polygon in red line).

4.2. Time series curve segmentation accuracy assessment

4.2.1. Parameter tuning for time series surface area curve segmentation method

To identify major lake surface area disturbances, the time series curve segmentation method removes small fluctuations but keeps major inflection points by setting thresholds for our curve segmentation method. There are two primary thresholding steps in our method, one for the D-P algorithm and the other for the bend simplification algorithm. Using a preset tolerance ε for D-P

Peer-reviewed version available at Remote Sens. 2020, 12, 612; doi:10.3390/rs12040612

algorithm and the angle threshold α, the time series curve will be segmented. The input data for the bend simplification algorithm are the data simplified by the D-P algorithm; therefore, it is especially important to select the threshold for the D-P algorithm. A high threshold for the D-P algorithm will result in important lake disturbance information losses, but a low threshold value will cause overfitting. Figure 4 shows the schematic diagram of the threshold selection for the time series curve segmentation, and panels 4(a), 4(b), 4(c), and 4(d) show the segmentation results from the D-P algorithm used with different thresholds. As shown in Figure 4, the threshold of 4(a) is too small and failed to reject most of the small variations that are not considered major disturbances. However, a high threshold value will result in the loss of major disturbances. Only the threshold of 0.06 set in panel 4(b) is reasonable in that it not only rejects several small variations but also maintains the major fluctuations.

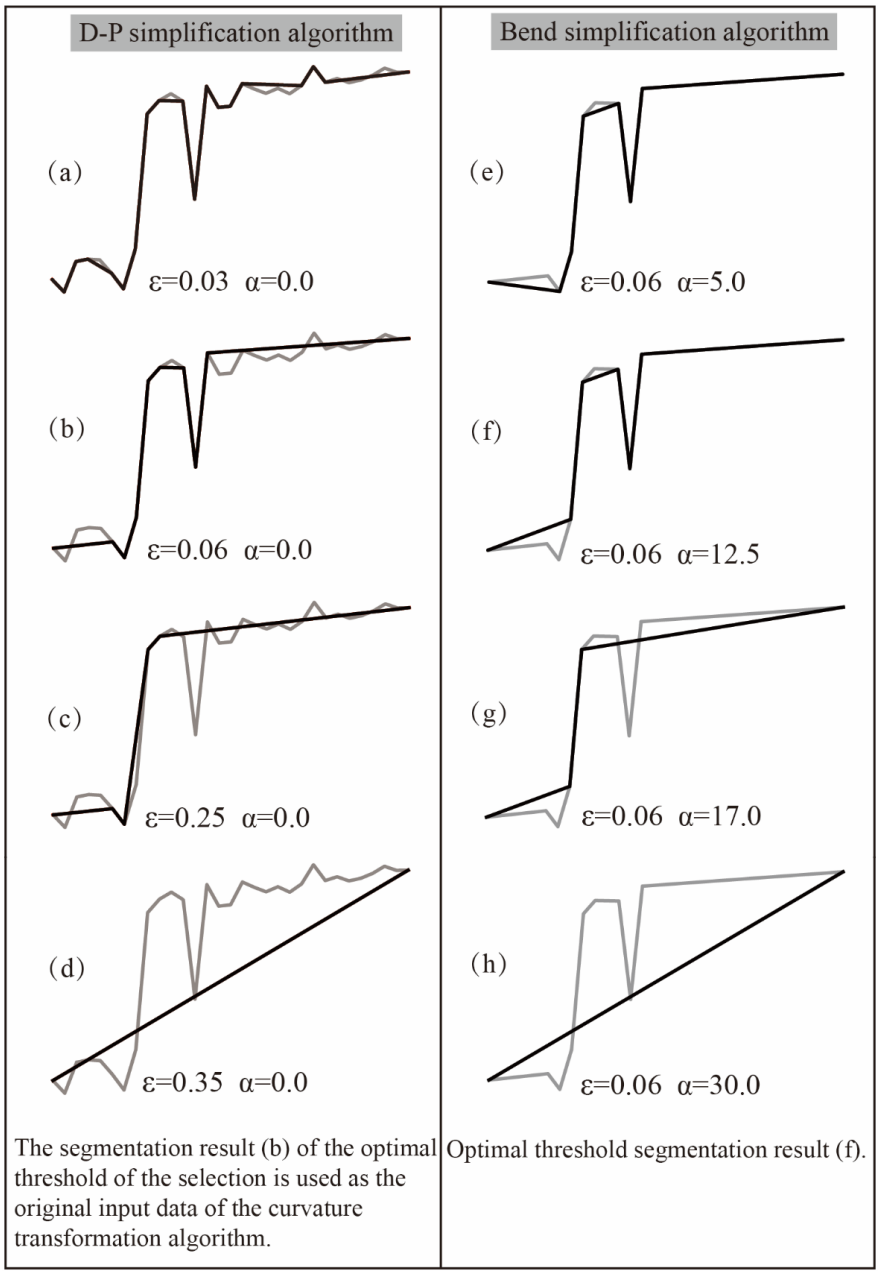

Figure 4. Selection of thresholds for the time series curve segmentation.

As there are still several small fluctuations not removed by the D-P simplification, the bend simplification algorithm is used to further simplify the segments obtained by the D-P algorithm. As

shown in Figure 4(e), when the threshold α for the bend simplification algorithm was too low, several small fluctuations were not eliminated. However, a greater threshold will cause several major disturbances to be eliminated, as shown in Figure 4(g) and 4(h). A threshold of 12.5 set in panel 4(f) is reasonable in that it not only maintains the large fluctuations but also rejects the small fluctuations. Thresholds used in this study are as listed in Table 4 for the D-P and bend simplification algorithms for segmenting the curves of the 9 lakes. For the D-P algorithm, the threshold was set to a value between 0.1 to 0.35 times the difference between the maximum and the minimum value on the curve. The threshold α for the bend simplification algorithm was set between 10° and 30° to obtain the optimum threshold.

Table 4. Tuning of time series curve segmentation parameters and their accuracies.

Lake	Maximum area(km²)	Minimum area(km²)	Area difference (km²)	Threshold ε for D-P	Threshold α for bend simplification
Shudu lake	1.7224	1.1853	0.5371	0.06	12.5
Qilu lake	46.4386	23.9597	22.4789	3.0	17.5
Yilong lake	43.2061	12.4935	30.7126	3.5	19.5
Bitahai lake	1.6434	1.5579	0.0855	0.03	23.0
Lashihai lake	13.1519	6.4716	6.6803	1.5	25.0
Yuxian lake	2.0114	0	2.0114	0.45	11.5
Haixihai lake	4.05	2.5017	1.5483	0.35	18.0
Dianchi lake	300.4219	293.9209	6.501	1.6	28.5
Erhai lake	244.9026	237.9613	6.9413	1.15	13.5

4.2.2 Time series curve segmentation results

The time series curve segmentation algorithm is key for identifying disturbances based on time series remote sensing observations [40]. However, noise caused by the lake surface extraction method, seasonal variation in the lake areas, random precipitation etc., in the time series curve is the main obstacle to time series curve-based analysis. Smoothing or simplification of a time series curve is needed to extract the features of disturbances from the curve [41].

After the D-P and bend simplification processing, segments that represent major lake surface disturbances are obtained; these segments indicate the duration, amplitude, beginning and ending time, etc., of each disturbance and are further used in the disturbance type classification. This is a key step for accurately identifying the disturbances; thus, the accuracy of the segmented segments has to be assessed prior to the classification step. This study used the simple and easy operational threshold determination method to simplify and segment the time series curves. As shown in Figure 5, the lake surface area time series curves of the 9 chosen lakes were segmented into 83 segments using our curve segmentation method and 21 records are marked in the results, indicating that our method could accurately locate these disturbances, including those from anthropogenic activities, such as reservoir constructions, irrigations, dam constructions, water storage projects, and natural factors, such as droughts and heavy rainfalls.

This study used yearly Landsat-extracted lake surface area data to construct the time series curve from 1987 to 2017; according to the 21 lake disturbance records, the 20 recorded disturbance dates are consistent with the segmentation results, for a total accuracy of 95.24%.

Preprints (www.preprints.org) | NOT PEER-REVIEWED | Posted: 30 December 2019 doi:10.20944/preprints201912.0392.v1

Peer-reviewed version available at Remote Sens. 2020, 12, 612; doi:10.3390/rs12040612

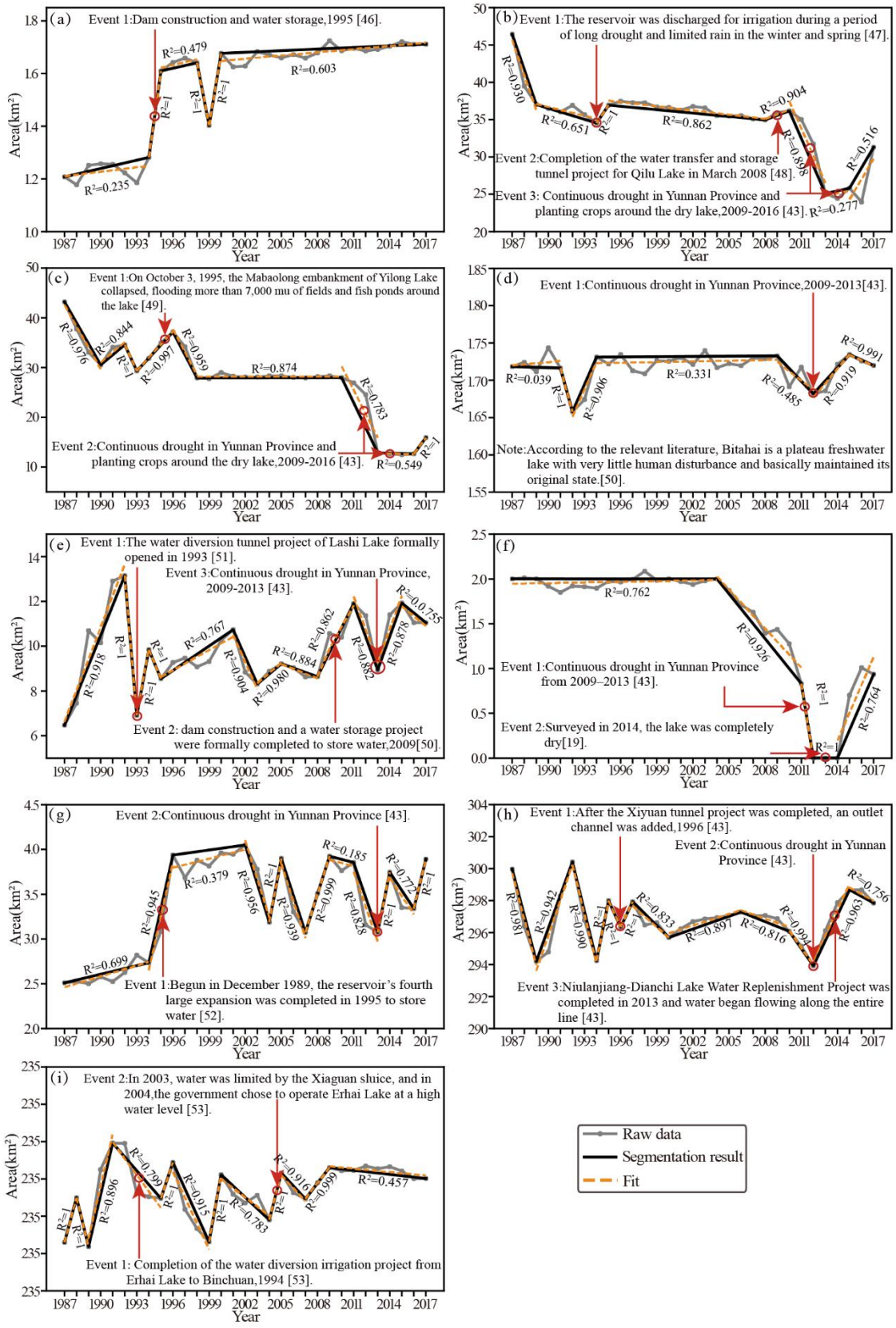

Figure 5. Time series curve segmentation and event identification results for lake areas in the study region during the period 1987–2017. Shudu Lake (a), Qilu Lake (b), Yilong Lake (c), Bitahai Lake (d), Lashihai Lake (e), Yuxian Lake(f), Haixihai Lake (g), Dianchi Lake (h), and Erhai Lake (i).

4.3. Lake surface area disturbance feature extraction and identification

4.3.1. Lake surface area disturbance feature extraction

Inland lakes vary in area and morphology; this is often the result of human activities or natural factors [42]. However, the temporal and spatial characteristics help distinguish these two kinds of lake surface area variations. To classify these major lake surface area changes into anthropogenic or natural events, we extracted the lake surface area features based on the segmented time series curves and their documented records. We found 21 officially documented lake change records for the 9 lakes (see Appendix 1); according to these references, anthropogenic lake surface area disturbances included reservoir constructions, irrigation, transforming lakes into fields, etc., and natural events included droughts, heavy rainfalls, etc.

Documented events and their characteristics of change on the time series curves are shown in Figure 5 and Appendix 1, and these distinguishable features can be summarized as follows: 1) human-induced lake surface area changes will cause an abrupt increase (or decrease) in the time series curve and the area increments are commonly larger for anthropogenic events compared to those for the natural disturbances, for example, due to anthropogenic activities, the lake surface area for Shudu Lake increased to 1.4 times that of 1993 between 1993 and 1995, the lake area of Lashihai Lake in 1993 increased to 2.03 times that of 1992, Yuxian Lake became 2.1 times larger in 2011 than it was 2006, and Haixihai Lake was in 1.4 times larger in area in 1996 than it was in 1994. In contrast, natural disturbances-induced lake area changes for Shudu Lake between 1998 and 1999, Bitahai Lake between 1990 and 1992, Lashihai Lake between 2010 and 2013, Haixihai Lake between 2010 and 2013 were 1.2, 1.1, 1.1, and 1.2 times the areas, respectively. The increased areas rarely revert to their original level in a short period of time (years) for these anthropogenic disturbances. 2) For natural disturbances, there are abrupt increases (or decreases) on the time series curves as well, but these increments (or decreases) decrease (or increase) to their original level at the end of a disturbance; therefore, these disturbances show a 'V' (or 'Λ') shape on the time series curves, and these natural event-caused changes typically consist of two parts, a change and a recovery, and the recovery is commonly missing from anthropogenic disturbances.

The 21 documented lake surface area disturbance events that we collected were randomly separated into two groups of samples; the first group of 9 events was used as a training sample to extract lakes disturbance features and to identify lake change type rules, and the second group of 12 events was used to validate the accuracy of the lake disturbance event type classification results. In this study, the documented disturbance records of Shudu Lake, Qilu Lake, Yilong Lake, Bitahai Lake and Lashihai Lake were used in integration with their curve segmentation results to extract lake change features, and the records of Yuxian Lake, Haixihai Lake, Dianchi Lake and Erhai Lake were used to validate and assess the accuracies of our lake change event identification method.

In this study, a total of 83 segments were generated for the 9 time series lake surface area curves; there was at least one major event for each of these lakes, either anthropogenic or natural. These disturbances caused remarkable fluctuations on the time series curves, and according to the shape of each fluctuation on the time series curves, fluctuations with remarkable durations indicate that there are close correlations between the current events and their adjacent procedures. Based on this characteristic of each disturbance and using these records as references, we define and extract the semantic features for each disturbance. Considering the adjacent procedure deficiency for disturbances segmented at the beginning or end of the curves, disturbances on the beginning or end of the curves were ignored. As a result, 65 disturbances (segments) in total were classified. Statistic results of the disturbances and their classes are shown in Appendix 1.

4.3.2. Classification results of lake surface area disturbances

According to the segmented curves, lake surface disturbance features such as the amplitude, trajectory, duration, and trends before and after a disturbance were extracted to classify each disturbance following an optimal decision rule. The amplitude was the ratio of the difference between

Peer-reviewed version available at Remote Sens. 2020, 12, 612; doi:10.3390/rs12040612

the area at the beginning of the segment and that at the end, and the difference between the maximum and the minimum area on the whole time series curve. Our statistical analysis of the documented records indicates that if this ratio is within the range [-0.11, 0.11], the corresponding disturbances are major disturbances, otherwise they are not major disturbances. For major disturbances, the documented records indicated that anthropogenic disturbances tend to not recover to their original level within a duration of approximately 3 years after a disturbance; however, natural disturbances had evident recover and mostly returned to their original levels. We quantify this recovery as the ratio between the beginning value of the previous segment and the ending value of the subsequent segment with the duration. The records for these recorded disturbances show that the anthropogenic disturbances had a recovery rate between 0.95 and 1.15 years, mostly within 3 years; otherwise, they were natural disturbances.

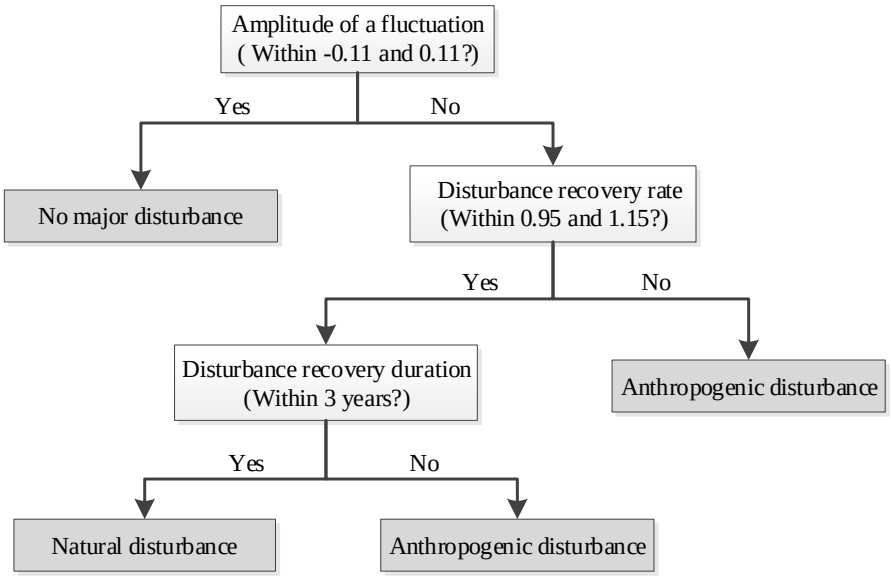

Figure 6. Classification tree to lake surface area disturbances.

Table 5. Statistics on the number of disturbances caused by different factors

Lake name	Anthropogenic disturbances (times)	Natural disturbances (times)	No disturbances	Total
Shudu lake	1	1	1	3
Qilu lake	4	0	2	6
Yilong lake	1	2	2	5
Bitahai lake	0	2	1	3
Lashihai lake	7	1	1	9
Yuxian lake	2	0	1	3
Haixihai lake	2	4	1	7
Dianchi lake	4	2	1	7
Erhai lake	7	2	0	9
Total	28	14	10	52

During the past 30 years, there were 42 major disturbances for the 9 lakes in Yunnan Plateau, and only 10 segments were with no major disturbances (see Figure 5 and Table 5). Among these disturbances, up to 28 were human-induced, and these disturbances had a major impact on lake surface area change. Human-induced disturbances are commonly 'irreversible', because lake surface area will not revert to its original levels within a short period of time; for example, lake surfaces for Shudu Lake between 1993 and 1995, Qilu Lake between 2010 and 2015, Yilong Lake between 2010 and 2016, Lashihai Lake between 1992 and 1993, Yuxian Lake between 2006 and 2011, and Haixihai

Lake between 1994 and 1996 increased (or decreased) to 1.4, 1.5, 2.2, 2.03, 2.1 and 1.4 times their original areas, respectively. Yuxian Lake completely dried between 2011 and 2014 because of human activities, including reclaiming land from this lake and irrigation [19][43]. These results indicated that the human-induced disturbances tend to be durable.

In our study period, natural event-induced major lake surface area disturbances occurred 14 times, half that of the human induced disturbances. These disturbances were far less impactful, because lake surface areas reverted to their original levels after these disturbances and, therefore, these disturbances were not long lasting. For example, natural disturbances for Shudu Lake between 1998 and 1999, Bitahai Lake between 1990 and 1992, Lashihai Lake between 2010 and 2013, and Haixihai Lake between 2010 and 2013, caused lake surface area increases (or decreases) to 1.2, 1.1, 1.1, and 1.2 times their original levels, respectively, and the lakes with natural disturbances had less of an increment (or decrement) compared to those with the human activity-induced disturbances, and they reverted to their original levels after a short period of time (within 2 years). In our study area, each of the lakes, except Bitahai Lake, had large human activity-induced disturbances, and there were much more anthropogenic disturbances for Lashihai Lake, Erhai Lake, Dianchi Lake and Qilu Lake. According to the documented records, most of these human activities were dam construction, irrigation, and land reclamation.

Disturbance identification accuracy was determined using the confusion matrix, which uses overall accuracy (OA) to represent the percentage of correctly classified disturbances, the user's accuracy (UA) to denote how well training-set samples are classified, and the producer's accuracy (PA) to show the probability that a classified sample represents a given class in reality [44]. In this study, we use UAad and UAnd to represent the user's accuracies of anthropogenic disturbances and natural disturbances and the PAda and PAnd to represent the producer's accuracies of anthropogenic disturbances and natural disturbances (see Table 6). We employed the method given by Adeline et al. [45] to evaluate the disturbances identification accuracy levels, and validation samples were randomly selected from the documented disturbance event records. Reference data and predicted results of the confusion matrix were defined as TP (true positive), TN (true negative), FP (false positive) and FN (false negative). TP denotes the number of correctly classified as anthropogenic disturbances, TN is the number of correctly detected as natural disturbances, FP represents the number of natural disturbances misclassified as anthropogenic disturbances, and FN is the number of anthropogenic disturbances misclassified as natural disturbances. As the F-score strikes a good balance between under- and overdetection accuracy levels, it is used in this study to evaluate the accuracy of the methods used (see Table 6).

Table 6. Classification accuracy assessment indices and formulas.

Producer's accuracy		User's accuracy			
Anthropogenic disturbances	**Natural disturbances**	**Anthropogenic disturbances**	**Natural disturbances**	**Overall accuracy**	**F-score**
$PA_{ad} = \frac{TP}{TP + FN}$	$PA_{nd} = \frac{TN}{TN + FP}$	$UA_{ad} = \frac{TP}{TP + FP}$	$UA_{nd} = \frac{TN}{FN + TN}$	$OA = \frac{TP + TN}{TP + TN + FP + FN}$	$F = 2\frac{PA_{ad}UA_{ad}}{PA_{ad} + UA_{ad}}$

Table 7. Disturbance identification accuracy assessment.

Producer's accuracy (%)		User's accuracy (%)				
Anthropogenic disturbances	**Natural disturbances**	**Anthropogenic disturbances**	**Natural disturbances**	**Overall accuracy**	**F(ad)-score**	**F(nd)-score**
100	75	88.89	100	91.67	94.67	85.71

The predicted disturbance types agreed well with the records according to the accuracy assessment results in Table 7; among the 12 recorded disturbances, only 1 natural disturbance was misclassified as an anthropogenic disturbance, and the overall identification accuracy was 91.67%,

with an F-score of 94.67 for anthropogenic disturbances and 85.71% for natural disturbances. This result suggests the reliability of our proposed method.

5. Conclusions

In this study, annual Landsat remote sensing images taken during the dry seasons from 1986 to 2017 were used to extract lake surface area information for 9 typical lakes in Yunnan Province, China. To identify whether human activity or natural events dominate inland lake surface change, we proposed a method based on the D-P simplification algorithm combined with the bend simplification method to locate large lake change events and then characterize the features of change for each event to classify them into anthropogenic or natural lake surface area disturbances. Based on validation data from a documented governmental report or year book, we assessed the accuracy of our method for both the disturbance location and the disturbance identification, and the results are as follows:

(1) The method can accurately locate the main lake changing events based on the time series lake surface area curve. When a large disturbance event occurs for a lake, its area will also increase (or decrease). The method proposed in this paper effectively eliminates noise in the time series of lake surface area using the combined D-P simplification algorithm and bend simplification algorithm. This method retains the large mutation points in the time series lake surface area curve and accurately locates the lake changing events within the time series lake surface curve; the temporal accuracy of this model for segmenting the lake area time series curves was 95.24% in our study.

(2) To characterize the disturbances on each time series curve, we extracted the disturbance classification features, including the amplitude, trajectory, duration, and trend before and after a disturbance. Combined with the CART decision tree classification method, we achieved an overall accuracy of disturbance identification of 91.67%, with an F-score of 94.67 for anthropogenic disturbances and 85.71% for natural disturbances.

(3) According to our results, lakes in Yunnan Provence, China, have undergone extensive disturbances, and the human-induced disturbances occurred almost twice as often as natural disturbances, indicating intensified disturbances caused by human activities, such as reservoir constructions, irrigation, turning lakes into fields, etc. Worse still, the anthropogenic disturbances appear to be lasting compared with the natural disturbances. Lakes subjected to natural disturbances tend to recover within a short period of time (3 years), while lakes subjected to anthropogenic disturbances had longer recovery times or never recovered.

Because the available remote sensing image data of satisfactory cloud-free quality from the study period are predominantly concentrated during Yunnan's dry season, the data selected were all from November to April. In future studies, multisensor spatial-temporal fusion techniques and radar remote sensing image data should be combined to obtain year-round lake water areas to comprehensively analyze the annual variation characteristics to more accurately capture lake disturbance events.

Author Contributions: Xiaolong Liu and Zhengtao Shi conceived and designed the study; Guangcai Huang analyzed the data, conducted the experiments and wrote the first draft of manuscript; Yanchen Bo and Guangjie Chen revised the manuscript; Xiaolong Liu and Zhengtao Shi finalized the manuscript.

Funding: This work was jointly supported by the National Key Research and Development Program of China (2016YFB0501502), the Applied Basic Research Project of Yunnan Province, China (Grant No. 2016FD021), the National Key Research and Development Program of China (Grant No. 2017YFA0605202).

Acknowledgments: We are thankful to the freely accessible Landsat and HJ-1A/B data by USGS and CRESDA. The authors would like to thank the reviewers for their constructive comments during the revision of this paper.

Conflicts of Interest: The authors declare no conflict of interest.

Preprints (www.preprints.org) | NOT PEER-REVIEWED | Posted: 30 December 2019 doi:10.20944/preprints201912.0392.v1

Peer-reviewed version available at Remote Sens. 2020, 12, 612; doi:10.3390/rs12040612

Appendix:

Appendix 1. Lake surface area change events and their semantic feature extraction results.

Event type	Lake	Year	Documented events	Year	Segmentation results and time series curve patterns	Semantic feature extraction
Human factors dominate lake disturbance events	Shudu lake	1995-	In 1995, the construction of the reservoir was completed and the reservoir was impounded.	1994-	After 1994, the lake area rapidly increased by a large margin, and in the following years; it keeps running at a higher water level.	Anthropogenic disturbances on time series curve tend to be: a. Abrupt increase (or decrease); b. With larger disturbance amplitude; c. Not recover within short period (3 years)
	Qilu lake	1993	The reservoir was discharged for irrigation during a period of long drought and limited rain in the winter and spring, 1993.	1989-1994	The lake area declined slightly from that of previous years.	
		2008-2010	Completion of the water transfer and storage tunnel project for Qilu Lake in March 2008.	2008-2010	The lake area increased from 2008–2010.	
		2009-2013	From 2009 to 2013, yunnan experienced a continuous drought, which increased the demand for agricultural water.	2010-2013	From 2010 to 2013, the lake area decreased rapidly.	
		2013-	From 2009 to 2013, during a drought in yunnan, villagers cultivated crops around the parched lake.	2013-	The lake area did not immediately recover after the drought ended in 2013.	
	Yilong lake	2009-2013	In 2009-2013, Yunnan Province continued to suffer from drought and agricultural water consumption has increased dramatically.	2010-2016	The lake area declined rapidly from 2010 to 2013.	
		2012-2015	Villagers reclaimed and planted along the dry lakeside	2013-2015	The drought ended, but the lake area did not recover, and the lake area had a "platform" from 2013 to 2016.	
Natural factors dominate lake disturbance	Yilong lake	1995	On October 3rd, 1995, the Mabaolong embankment of Yilong Lake collapsed, flooding more than 7,000 mu of fields and fish ponds around the lake.	1993-1996	The lake area increased rapidly and reached a high value in 1995-1996, followed by a rapid decline in the following two years.	Natural disturbances on time series curve tend to show: a. An abrupt increase (or decrease); b. A smaller disturbance amplitude compared to those from anthropogenic disturbances; c. Recovery within short period (3 years), and the trajectory of a natural disturbance on the time series curve will be in "V" or "Λ" shape.
	Bitahai lake	2009-2013	Yunnan Province continued to suffer from drought, 2009-2013	2010-2013	In 2010-2013, the lake area declined and then rose back to the previous year's water level.	
	Lashihai lake	2009-2013	Yunnan Province continued to suffer from drought, 2009-2013	2010-2013	In 2009-2013, the lake area declined rapidly and then quickly rose back to the previous year's water level.	

References

1. Ding, Y.; Liu, S.; Ma, Y.; Ye, B.; Zhao, L. Climatic implications on variations of lakes in the cold and arid regions of china during the recent 50 Years. *Journal of Glaciology and Geocryology*. **2006**, *28(5)*, 623-632. DOI: 10.1007/s11442-006-0415-5
2. Pekel, J. F., Cottam, A., Gorelick, N., Belward, A. S. High-resolution mapping of global surface water and its long-term changes. *Nature*. **2016**, *540(7633)*, 418-422. doi:10.1038/nature20584
3. Yamazaki, D., Trigg, M. A., Ikeshima, D. Development of a global ~90m water body map using multi-temporal Landsat images. *Remote Sensing of Environment*. **2015**, *171*, 337-351. DOI:10.1016/j.rse.2015.10.014
4. Moser, K. A., Baron, J. S., Brahney, J., Oleksy, I. A., Saros, J. E., Hundey, E. J.,et al. Mountain lakes: Eyes on global environmental change. *Global and Planetary Change*. **2019**, *178*, 77-95. DOI: 10.1016/j.gloplacha.2019.04.001
5. Vorosmarty, C. J., Green, P., Salisbury, J., Lammers, R. B. Global water resources: vulnerability from climate change and population growth. *Science*. **2000**, *289(5477)*, 284-288. DOI:10.1126/science.289.5477.284
6. Huang, C., Chen, Y., Zhang, S., Wu, J. Detecting, extracting and monitoring surface water from space using optical sensors: a review. *Reviews of Geophysics*. **2018a**, *56(2)*, 333-360. DOI: 10.1029/2018RG000598
7. Luo, K. S., Tao, F. L. Monitoring of forest virtual water in Hunan Province, China, based on HJ-CCD remote-sensing images and pattern analysis. *Internationl Journal of Remote Sensing*. **2016**, *37(10)*, 2376-2393. DOI: 10.1080/01431161.2016.1176275
8. Tulbure, M. G., Broich, M., Stehman, S. V., Kommareddy, A. Surface water extent dynamics from three decades of seasonally continuous Landsat time series at subcontinental scale in a semi-arid region. *Remote Sensing of Environment*. **2016**, *178*, 142-157. DOI:10.1016/j.rse.2016.02.034
9. Feng, L., Hou, X., Zheng, Y. Monitoring and understanding the water transparency changes of fifty large lakes on the Yangtze Plain based on long-term MODIS observations. *Remote Sensing of Environment*. **2019**, *221*, 675-686. DOI: 10.1016/j.rse.2018.12.007
10. Peng, J., Jia, J., Liu, Y., Li, H., Wu, J. Seasonal contrast of the dominant factors for spatial distribution of land surface temperature in urban areas. *Remote Sensing of Environment*. **2018**, *215*, 255-267. DOI:10.1016/j.rse.2018.06.010
11. Che, X., Feng, M., Jiang, H., Xiao, T., Wang, C., Jia, B., Bai, Y. Detection and analysis of Qinghai-Tibet Plateau lake area from 2000 to 2013. *Journal of Geo-information Science*. **2015**, *17(1)*, 97-107. DOI: 10.3724/SP.J.1047.2015.00099
12. Mcfeeters, S. K. The use of the Normalized Difference Water Index (NDWI) in the delineation of open water features. *International Journal of Remote Sensing*. **1996**, *17(7)*, 1425-1432. DOI: 10.1080/01431169608948714
13. Feng, L., Hu, C. M., Chen, X. L., Cai, X. B., Tian, L. Q., Gan, W. X. Assessment of inundation changes of Poyang Lake using MODIS observations between 2000 and 2010. *Remote Sensing of Environment*. **2012**, *121(2)*, 80-92. DOI: 10.1016/j.rse.2012.01.014
14. Li, H. Y., Mao, D. H., Li, X. Y., Wang, Z. M., Wang, Z. M., Wang, C. Z., 2019. Monitoring 40-year lake area changes of the Qaidam Basin, Tibetan Plateau, using Landsat time series. *Remote Sensing*. *11(3)*. DOI:10.3390/rs11030343
15. Maeda, E. E., Lisboa, F., Kaikkonen, L., Kallio, K., Koponen, S., Brotas, V., Kuikka, S. Temporal patterns of phytoplankton phenology across high latitude lakes unveiled by long-term time series of satellite data. *Remote Sensing of Environment*. **2019**, *221*, 609-620. DOI:10.1016/j.rse.2018.12.006
16. Wulder, M. A., Loveland, T. R., Roy, D. P., Crawford, C. J., Masek, J. G., Woodcock, C. E., Zhu, Z. Current status of Landsat program, science, and applications. *Remote Sensing of Environment*. **2019**, *225*, 127-147. DOI:10.1016/j.rse.2019.02.015
17. Xiao, Q., Yang, K., Hong, L. Remote sensing monitoring and temporal-spatial analysis of surface water body area changes of lakes on the Yunnan-Guizhou Plateau over the past 30 years. *Jouranal of Lake Sciences*. **2018**, *30(4)*, 1083-1096. DOI: CNKI:SUN:FLKX.0.2018-04-022
18. Arvor, D., Daher, F. R. G., Briand, D., Dufour, S., Rollet, A. J., Simoes, M., Ferraz, R. P. D. Monitoring thirty years of small water reservoirs proliferation in the southern Brazilian Amazon with Landsat time series. *ISPRS Journal of Photogrammetry and Remote Sensing*. **2018**, *145*, 225-237. DOI: 10.1016/j.isprsjprs.2018.03.015
19. Li, H., Zhang, H., Chen, G., Chang, F., Duan, L., Wang., Lu,H.,et al. The Grain Size Distribution Characteristics of Surface Sediments from Plateau Lakes in Yunnan Province and Their Environmental Significances. *Acta Sedimentologica Sinica*. **2017**, *03*, 78-86. DOI: CNKI:SUN:CJXB.0.2017-03-008

20. Qin, J., Ju, J., Xie, M. Low Latitude Plateau Weather Climate. China Meteorological Press. **1997**, 18-19.
21. Cooley, T., Anderson, G. P., Felde, G. W., Hoke, M. L., Ratkowski, A. J., Chetwynd, J. H., et al. FLAASH, a MODTRAN4-based atmospheric correction algorithm, its application and validation. *IEEE International Geoscience and Remote Sensing Symposium. IEEE*. **2002**. DOI: 10.1109/IGARSS.2002.1026134
22. Zhu, Z., Woodcock, C. E. Object-based cloud and cloud shadow detection in Landsat imagery. *Remote Sensing of Environment*. **2012**, *118*, 83-94. DOI:10.1016/j.rse.2011.10.028
23. Wang, M., Du, L., Ke, Y., Huang, M., Zhang, J., Zhao, Y., et al. Impact of Climate Variabilities and Human Activities on Surface Water Extents in Reservoirs of Yongding River Basin, China, from 1985 to 2016 Based on Landsat Observations and Time Series Analysis. *Remote Sensing*, **2019**, *11(5)*, 560. DOI: 10.3390/rs11050560
24. Douglas, D. H., Peucker, T. K. Algorithms for the Reduction of the Number of Points Required to Represent a Digitized Line or its Caricature. *Classics in Cartography. Cartographica: The International Journal for Geographic Information and Geovisualization*. **1973**, *10(2)*, 112-122. DOI: 10.1002/9780470669488.ch2
25. Wang, Z., Müller, J. C. Line generalization based on analysis of shape characteristics. *Cartography and Geographic Information Systems*, **1998**, *25(1)*, 3-15.
26. Frazier, P. S. Water body detection and delineation with Landsat TM data. *Photogrammetric Engineering and Remote Sensing*. **2000**, *66(12)*, 1461-1467. DOI: 10.1016/S1361-8415(00)00023-2
27. Feyisa, G. L., Meilby, H., Fensholt, R., Proud, S. R. Automated water extraction index: a new technique for surface water mapping using Landsat imagery. *Remote Sensing of Environment*. **2014**, *140(1)*, 23-35. DOI:10.1016/j.rse.2013.08.029
28. Huang, X., Hu, T., Li, J., Wang, Q., Benediktsson, J. A. Mapping urban areas in China using multisource data with a novel ensemble SVM method. *IEEE Transactions on Geoscience and Remote Sensing*. **2018b**, *56(8)*, 4258-4273. DOI:10.1109/tgrs.2018.2805829
29. Fisher, A., Flood, N., Danaher, T. Comparing Landsat water index methods for automated water classification in eastern Australia. *Remote Sensing of Environment*. **2016**, *175*, 167-182. DOI:10.1016/j.rse.2015.12.055
30. Otsu, N. A Threshold Selection Method from Gray-Level Histograms. *IEEE Transactions on Systems Man and Cybernetics*. **1979**, *9(1)*, 62-66. DOI: 10.1109/tsmc.1979.4310076
31. Xu, H. Modification of normalised difference water index (NDWI) to enhance open water features in remotely sensed imagery. *International Journal of Remote Sensing*. **2006**, *27(14)*, 3025-3033. DOI: 10.1080/01431160600589179
32. Sun, G., Chen, X., Jia, C., Yao, Y., Wang, Z. Combinational Build-Up Index (CBI) for effective impervious surface mapping in urban areas. *IEEE Journal of Selected Topics in Applied Earth Observations and Remote Sensing*. **2016**, *9(5)*, 2081-2092. DOI: 10.1109/JSTARS.2015.2478914
33. Kennedy, R. E., Yang, Z., Cohen, W. B. Detecting trends in forest disturbance and recovery using yearly Landsat time series: 1. LandTrendr - Temporal segmentation algorithms. *Remote Sensing of Environment*. **2010**, *114(12)*, 2897-2910. DOI:10.1016/j.rse.2010.07.008
34. Zhu, Z., Woodcock, C. E. Continuous change detection and classification of land cover using all available Landsat data. *Remote Sensing of Environment*, **2014**, *144*, 152-171. DOI: 10.1016/j.rse.2014.01.011
35. Verbesselt, J., Hyndman, R., Newnham, G., Culvenor, D. Detecting trend and seasonal changes in satellite image time series. *Remote Sensing of Environment*. **2010**, *114(1)*, 106-115. DOI: 10.1016/j.rse.2009.08.014
36. Chuon, C., Guha, S., Janecek, P., Nguyen, D.C.S. Simplipoly: curvature-based polygonal curve simplification. *International Journal of Computational Geometry and Applications*. **2011**, *21(04)*, 417-429. DOI: 10.1142/S0218195911003743
37. Breiman, L. Classification and regression trees: Routledge, 2017.
38. Timofeev, R. Classification and regression trees (CART) theory and applications. Humboldt University, Berlin, 2004.
39. Zeng, L., Schmitt, M., Li, L., Zhu, X. Analysing changes of the Poyang Lake water area using Sentinel-1 synthetic aperture radar imagery. *International Journal of Remote Sensing*. **2017,** *38(23)*, 7041-7069. DOI: 10.1080/01431161.2017.1370151
40. Sulla-Menashe, D.; Kennedy, R.E.; Yang, Z.; Braaten, J.; Krankina, O.N.; Friedl, M.A. Detecting forest disturbance in the Pacific Northwest from MODIS time series using temporal segmentation. *Remote Sensing of Environment*. **2014**, 151, 114-123, doi:10.1016/j.rse.2013.07.042.

41. Liu, X.; Bo, Y.; Zhang, J.; He, Y. Classification of C3 and C4 Vegetation Types Using MODIS and ETM+ Blended High Spatio-Temporal Resolution Data. *Remote Sensing*. **2015**, 7, 15244-15268, doi:10.3390/rs71115244.
42. Goudie, A. S. Human Impact on the Natural Environment: Wiley, 2018.
43. He, J. Yunnan Water Conservancy Yearbook. Yunnan Water Resources Department, Kunming China, 2014.
44. Congalton, R. G. A review of assessing the accuracy of classifications of remotely sensed data. *Remote Sensing of environment*. **1991**, 37(1), *35-46*. DOI: 10.1046/j.1365-2249.2000.01137.x
45. Adeline, K. R. M., Chen, M., Briottet, X., Pang, S. K., Paparoditis, N. Shadow detection in very high spatial resolution aerial images: A comparative study. *ISPRS Journal of Photogrammetry and Remote Sensing*. **2013**, *80*, 21-38. DOI: 10.1016/j.isprsjprs.2013.02.003
46. Li, H., Yu, Q., Li, N., Wang, J., Yang, Y. Study on Landscape Dynamics and Driving Mechanisms of the Shudu Lake Catchment Wetlands in Northwest Yunnan. *Journal of West China Forestry Science*. **2013**, *42(3)*. DOI:10.16473/j.cnki.xblykx1972.2013.03.003
47. Gong, P. Huaning Water Conservancy. Dehong National Publishing House, Mangshi, 2014
48. Duan, Z. Tonghai Yearbook. Dehong National Publishing House, Dehong China, 2013.
49. Compilation of Shiping County annals Compilation Committee. Shiping County annals: 1985-2000. Yunnan People's Publishing House, Kunming China, 2005.
50. Yang, L., Li, H. Yunnan wetland. China Forestry Publishing House, Beijing China, 2010.
51. Li, R. Annals of Naxi Autonomous County of Lijiang. Yunnan People's Publishing House, Kunming China, 2001.
52. Compilation of Eryuan County Local Chronicles Compilation Committee. Eryuan County records: 1978-2005. Yunnan People's Publishing House, Kunming China, 2018.
53. Yan, S. Discussion on the Environmental Impact of Erhai Sea Engineering Construction. *Technological Development of Enterprise*. **2014**, *33(9)* DOI: 10.3969/j.issn.1006-8937.2014.06.026